

## MODELLING OF ELECTROMECHANICAL CONVERTERS OF TRACTION USED ON ELECTRIC LOCOMOTIVES

Doru Adrian NICOLA, Daniel Cristian CISMARU

UNIVERSITY OF CRAIOVA, email: dnicola@em.ucv.ro, dcismaru@em.ucv.ro

**Abstract** – The paper begins by presenting basic electrical diagrams of the main types of electric locomotives (with chopper and DC motors or with rectifiers and DC motors or with VVVF and induction motors IM or with self-controlled synchronous motors SCSM) powered from DC contact line or from AC contact line. To obtain the movement diagrams, in the paper they are established the equations of useful movement and it is built the structural diagram corresponding to a locomotive with „z” traction identical motors. The paper aims to build, on the new concepts basis, structural models (easily reconfigurable in the Simulink models) for all types on electromechanical converters, of traction, that are today installed on the electric locomotives. For modelling is proposed the original idea of fictitious split of any traction electric motors into an „electromagnetic part” and into a „mechanical part”. Construction differences, functional differences and mathematical differences of the equations that describing the various types of electromechanical converters are given only by their electromagnetic parts. Starting from that idea, the paper presents the mathematical equations and structural diagrams for all electromechanical converters of traction used on the electric locomotives. For electromagnetic part of the DC motors and the induction motors, equations and structural diagrams take into account the real iron core magnetization curve. Only for modeling SM is adopted the Park theory (with unsaturated iron core). As a validation of the models, in the last part of the paper are summarized the Simulink model of an induction motor, the Simulink model for useful movement and, for concrete data, the running diagrams of ETR 500 high speed train obtained by numerical simulation.

**Keywords:** *Electric Locomotives, Modelling, Structural Diagram, Electromechanical Converters*

### 1. INTRODUCTION

Electric locomotives with DC motors [1], [2], [3] [4] have configuration of main electric circuit dependent by voltage (DC or AC) of the contact line. From this point of view we distinguish two basic structures:

- a basic configuration (as in Fig. 1) corresponding to electric locomotives with chopper and DC motors powered from the DC contact line (LC) of 1.5 kV or 3 kV and

- a basic configuration (as in Fig. 2) corresponding to electric locomotives (with rectifiers and DC motors)

fed from AC the contact line (LC) of 15 kV and 16 $\frac{2}{3}$  Hz or 25 kV and 50/60 Hz.

Electric locomotives equipped with DC motors fed from DC line (Fig. 1) have a  $L_F C_F$  network filter (usually in  $\Gamma$ ), only one regardless of the number of the dc choppers. If the electric locomotives (with DC motors) are fed from AC contact line (like in Fig. 2), both autotransformer (AT) and main traction transformer (TP) are unique, regardless of the number of rectifiers.

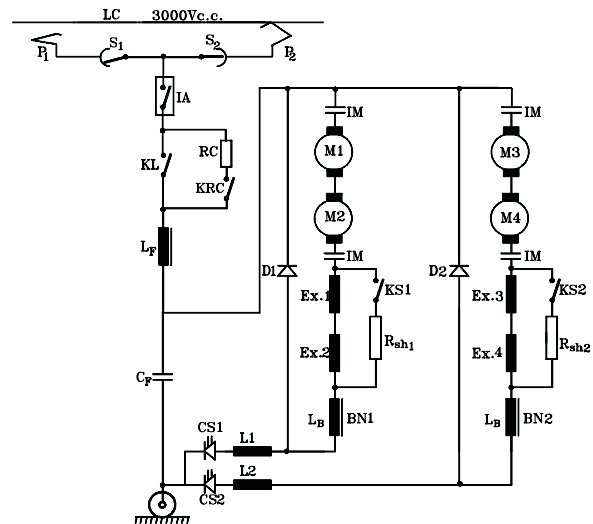


Figure 1: Electric locomotives with chopper and DC motors

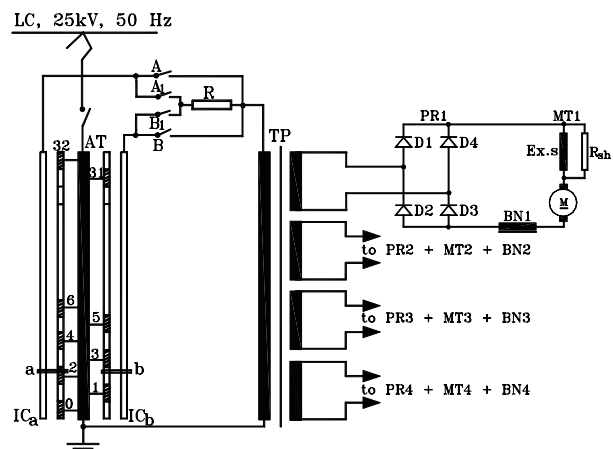


Figure 2: Electric locomotives with rectifiers and DC motors

In both cases, for limiting the load current corrugations of the dc motor are used, in series, BN coils (with saturated iron core).

From last two decades of the XX century has started the using of the three-phase induction motor (with squirrel cage) as traction motor [4], [5], [6], [7], [8]. Use of induction motor on electric locomotives was possible only after providing a three phase power-supply, with variable voltage and variable frequency (VVVF) inverters (IT with 2 or 3 levels).

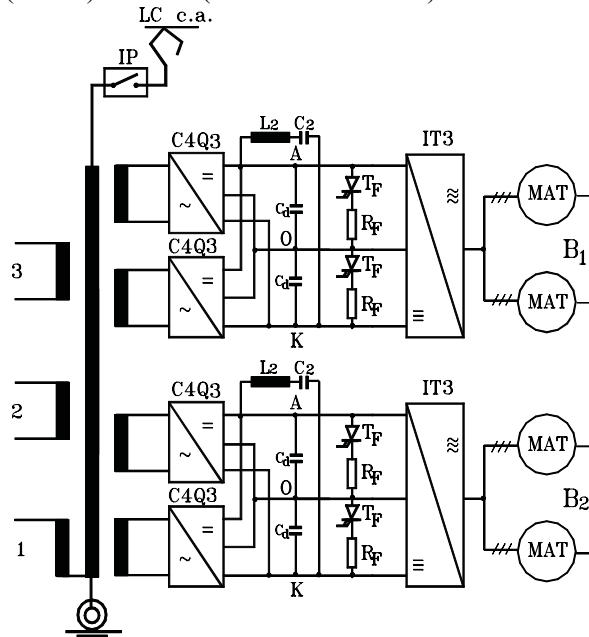


Figure 3: Electric locomotives with C4Q, VVVF and IM

Electric locomotives with induction motors of traction (MAT) supplied by the AC contact line (at 15 kV and 16 2/3 Hz or at 25 kV 50/60 Hz) are exclusively equipped with four quadrant converters C4Q with 2 or 3 levels (on the line-side) and powered by the VVVF inverter (IT inverters with 2 or 3 levels) on the machine-side (Fig. 3).

Electric locomotives with induction traction motors (MAT) supplied by the DC contact line (at 1.5 kV or

3.0 kV) have dc chopper of 2Q and / or only VVVF power inverters (IT with 2 or 3 levels), as in Fig. 4.

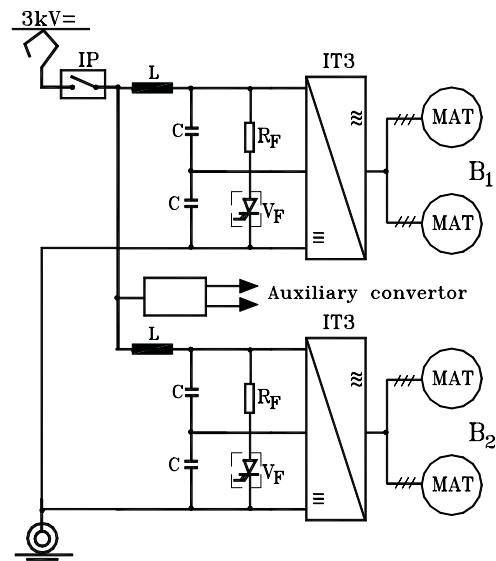


Figure 4: Electric locomotives with VVVF and IM

By replacing the dc traction motors (with commutator) from Fig.1 (or Fig.2) with self-controlled synchronous motors (SCSM, Fig. 5) we obtain a new configuration for main electric circuit of the electric locomotives (like as TGV) [2], [3], [4], [5],[8].

The paper aims to build, on the new concepts basis, new structural models (easily reconfigurable in the Simulink models) for all types of the electromechanical converters, of traction, that are today installed on electric locomotives.

## 2. MODELLING OF USEFUL MOVEMENT

Useful movement is the effect of the electromagnetic torques of traction motors. Mathematical model of useful motion of a locomotive (with “z” traction identical motors) it is described by the next equations [1], [3], [9]:

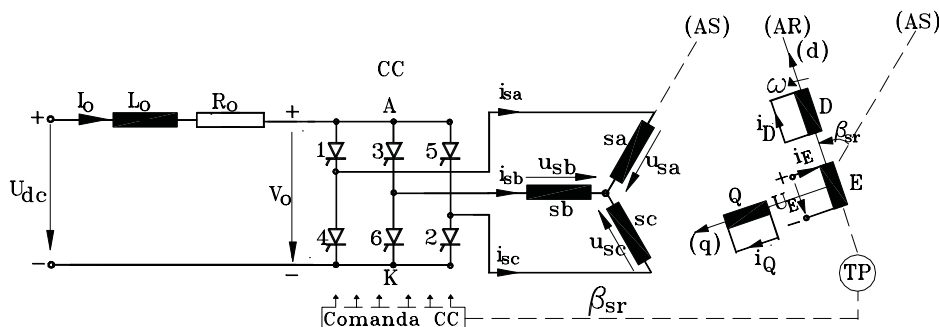


Figure 5: Self-controlled synchronous motor (SCSM)

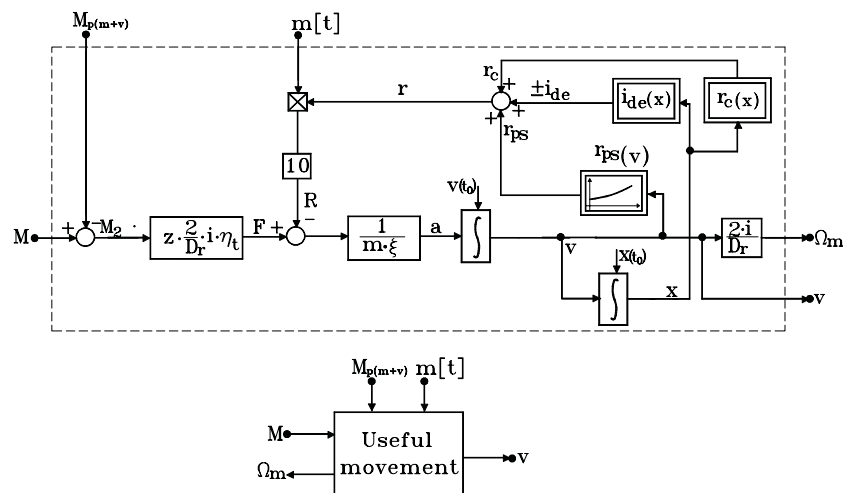


Figure 6: Structural diagram of useful movement

$$\begin{aligned}
 v(t) &= \frac{1}{m \cdot \xi} \int_0^t (F-R) dt + v(t_0); \quad \Omega_m = \frac{2 \cdot i}{D_r} \cdot v; \\
 x(t) &= \int_0^t v \cdot dt + x(t_0); \quad F = z \cdot \frac{2}{D_r} \cdot i \cdot \eta_t \cdot M_2; \\
 R &= [r_{ps}(v) \pm i_{de}(x) + r_c(x)] \cdot m \cdot 10
 \end{aligned}
 \tag{1}$$

where (for a single traction motor)  $M_2 = M - M_{p(m+v)}$ . These equations, have permitted construction of the structural diagram [1] as in Fig.6.

Changing mass “m” of the train, the dependencies  $i_{de}(x)$  and  $r_c(x)$  or specific train route can be easily operated, each time achieving mathematical models that fully respects the concrete conditions of work.

### 3. MODELLING OF DC MOTORS

For modelling of the DC motors will be imagined a "breakdown" as in Fig. 7 [1], [3], [9]. For the electromagnetic subsystem, the input variable is  $U_M$  voltage. Output variable is electromagnetic torque  $M$  of the dc motor. Main magnetic flux  $\Phi$  is an internal variable and not appear explicitly in the scheme of decomposition. The mechanical part has at input the electromagnetic torque  $M$  and at output the angular velocity of rotation  $\Omega$  (of the rotor). In the same time, the

electromagnetic torque  $M$  and angular velocity  $\Omega$  are variables of internal interaction between the two subsystems of dc motor.

Because that mechanical parts of the dc motors of traction have been included in the model of useful movement, still to be determined only complete model of the electromagnetic subsystem for the two types of DC motors (with series excitation and with independent excitation) of traction.

#### 3.1 Modelling Electromagnetic Part of a dc Motor with Serie Excitation

Mathematically, the armature winding is represented by circuit parameters  $R_a$ ,  $L_a$  and average value of the internal emf  $E$ . On these conditions, the equation for the armature circuit, the emf  $E$  and the electromagnetic torque  $M$  can be write in the form [1], [3], [10], [11]:

$$\begin{aligned}
 \frac{dI_a}{dt} &= \frac{1}{L_a} [U_a - R_a \cdot I_a - E] \\
 E &= C_m \cdot \phi \cdot \Omega \\
 M &= C_m \cdot \phi \cdot I_a
 \end{aligned}
 \tag{2}$$

where  $C_m = \frac{1}{2\pi} \cdot \frac{p \cdot N}{a}$  is the constant of the machine.

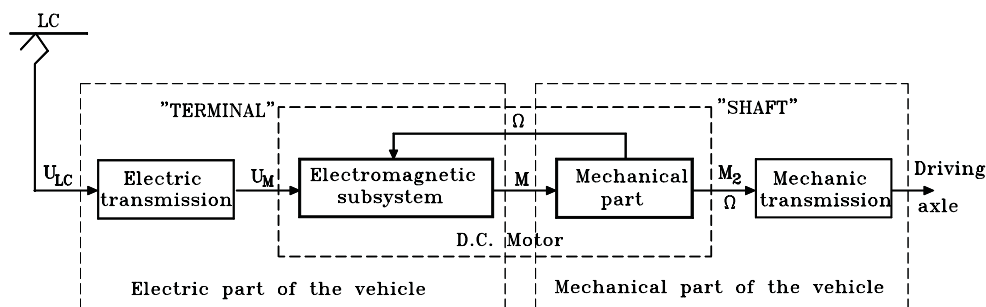


Figure 7: The "decomposition" of dc motor

For a serie dc motor we have  $I_e = I_a$ . Instead, voltage  $U_e$  is determined in conjunction with the magnetic field and with the parameters of excitation winding by the following equations [1], [3] :

$$\begin{aligned}
 I_e &= I_a; \quad \phi = \phi(I_e) \\
 \phi_e &= \phi + \sigma_e \cdot \frac{\phi_n}{I_{en}} \cdot I_e \\
 \psi_e &= 2p \cdot w_{ex} \cdot \phi_e \\
 U_e &= R_e \cdot I_e + \frac{d\psi_e}{dt}
 \end{aligned}
 \tag{3}$$

Equations (2) and (3) with  $U_a = U_M - U_e$  form the mathematical model for DC motor with serie excitation. On basis of those equations it was represented the structural diagram as in fig.8. The only input variable is the voltage  $U_M$ . Rotor angular velocity  $\Omega$  is an internal variable of the traction motor. The output variables are  $M$  and  $I_a$ .

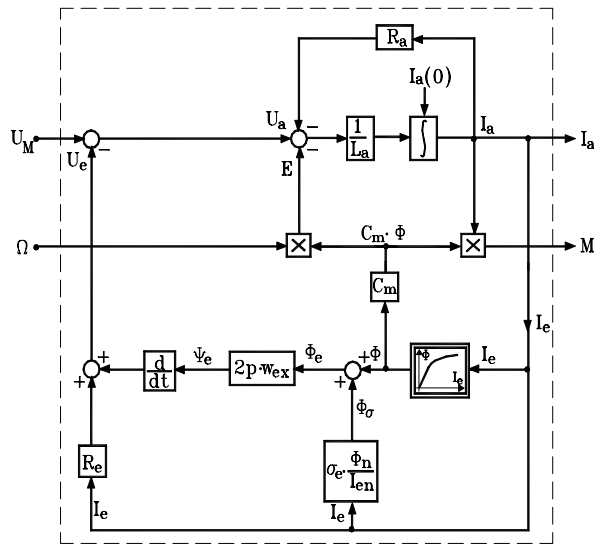


Figure 8: Structural diagram for the electromagnetic subsystem of the serie dc motor

### 3.2 Modelling Electromagnetic Part of a dc Motor with Independent Excitation

The armature will be described by the equations (2). Instead, at independent fed (with voltage  $U_e$ ) the field winding equations are [1], [3], [10], [11]:

$$\begin{aligned}
 \psi_e &= \int_0^t (U_e - R_e \cdot I_e) dt + \psi_e(0) \\
 \phi_e &= \frac{\psi_e}{2p \cdot w_{ex}} \\
 \phi &= \phi_e - \sigma_e \cdot \frac{\phi_n}{I_{en}} \cdot I_e \\
 I_e &= f^{-1}(\phi)
 \end{aligned}
 \tag{4}$$

Here  $I_e = f^{-1}(\phi)$  functional means "reverse" of magnetization curve of the magnetic iron core.

Ensemble equations (2) and (4) represent mathematical model for a dc motor with independent excitation. By graphic representation, with symbols, they lead [1], [3] to the structural diagram as in Fig.9. Here, armature winding and field winding are only coupled by the magnetic field.

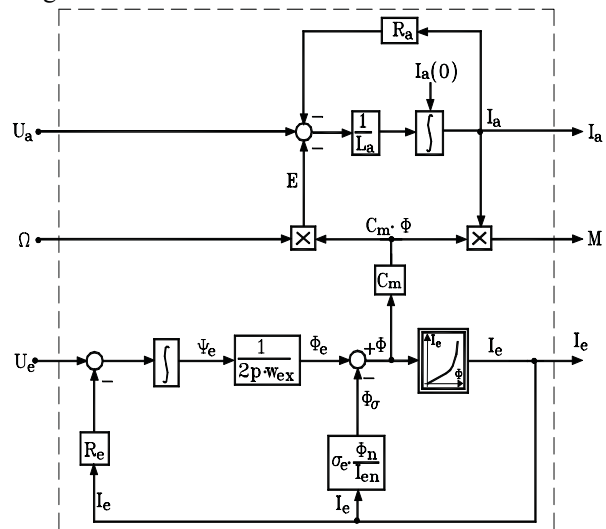


Figure 9: Structural diagram for the electromagnetic subsystem of the dc motor with independent excitation

The structural diagram has two input variables:  $U_a$  and  $U_e$ . Here  $\Omega$  is the internal variable of the dc motor. Instead, output variables are in number of three, namely: armature current  $I_a$ , field current  $I_e$  and electromagnetic torque  $M$ .

### 4. MODELLING OF INDUCTION MOTOR

For the modelling, is judiciously as the induction motor of traction IM (or the asynchronous

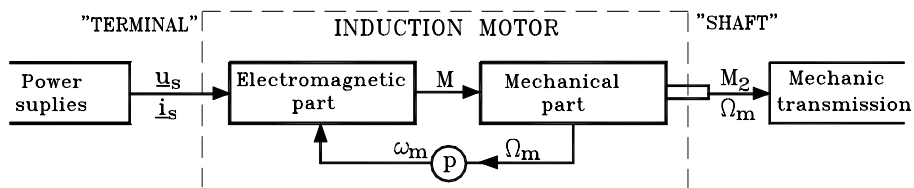


Figure 10: The "decomposition" of induction motor of traction (MAT)

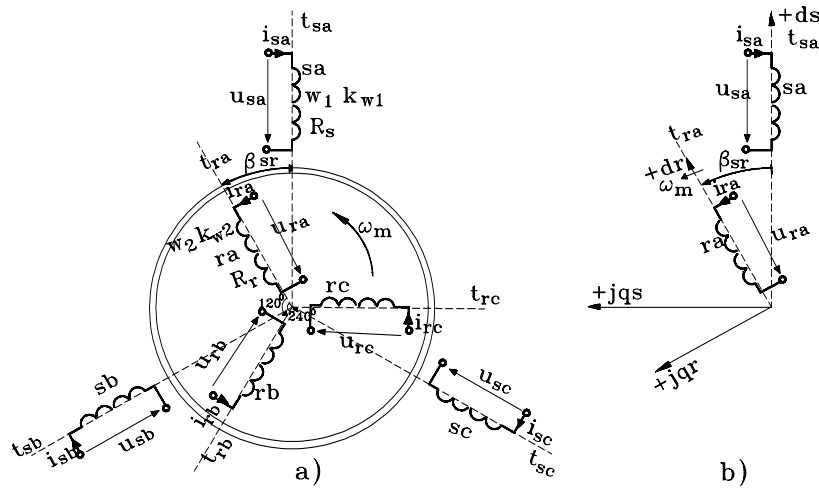


Figure 11: Electromagnetic part of induction motor

electromechanical converter MAT in fig.3 and fig.4) to be formally split into an „electromagnetic part” and a „mechanical part”, parts connected together by internal variables  $M$  and  $\omega_m = p \cdot \Omega_m$  as in Fig.10 [3], [12], [13].

The mechanical part of the induction motor of traction (through the mass of rotor, by considering of the  $J$  in to constant inertia  $\xi = 1 + \gamma$  and by considering the torques  $M$  and  $M_{p(m+v)}$ ) has been already integrated in the mechanical part of the locomotive and mathematically it was included in the equations of useful movement with structural diagram in Fig.6. The electromagnetic part of an induction motor of traction is governed by general laws of the electromagnetic field. For modeling, will consider the model from Fig.11. As working method is adopted the space phasors method [10], [11], [12], [13], [14], [15].

In the electromagnetic model will consider that core saturation affects only the  $\Psi_u$  value of the useful magnetic flux. The leakages flux are not influenced by saturation and thus can be written in the forms:

$$\underline{\Psi}_{s\sigma} = L_{s\sigma} \cdot \underline{i}_{ss} \quad \text{and} \quad \underline{\Psi}'_{r\sigma} = L'_{r\sigma} \cdot \underline{i}'_{rs}$$

The equations of a symmetrical electromagnetic part of an induction motor in the stator reference frame can be summarized [10], [13], [14], [15] in the form:

$$\begin{aligned} \underline{u}_{ss} &= R_s \cdot \underline{i}_{ss} + \frac{d\underline{\Psi}_{ss}}{dt} \\ 0 &= R'_r \cdot \underline{i}'_{rs} + \frac{d\underline{\Psi}'_{rs}}{dt} - j \cdot \omega_m \cdot \underline{\Psi}'_{rs} \end{aligned} \quad (5)$$

$$\underline{\Psi}_{ss} = L_{s\sigma} \cdot \underline{i}_{ss} + \underline{\Psi}_{us}$$

$$\underline{\Psi}'_{rs} = L'_{r\sigma} \cdot \underline{i}'_{rs} + \underline{\Psi}_{us}$$

$$\underline{i}_{ss} + \underline{i}'_{rs} = \underline{i}_{-s}; \quad \Psi_u = \Psi_u(i_{-s})$$

$$M = \frac{3}{2} \cdot p \cdot \text{Im} \{ \underline{i}_{-s} \cdot \underline{\Psi}_{ss}^* \}; \quad \omega_m = p \cdot \Omega_m$$

Due to the symmetry of the magnetic core will work with a single magnetization curve  $\Phi_u = \Phi_u(i_{-s})$ . Useful

flux linkage  $\Psi_u = \Psi_{f1}$  is determined by the relationship  $\Psi_u = w_1 \cdot k_{w1} \cdot \Phi_u$ . At neglecting the iron losses, the phasors  $\underline{\Psi}_{us}$  și  $\underline{i}_{us}$  will keep same direction. Mathematically we can write:

$$\begin{aligned} i_{-s} &= \text{Abs} \{ \underline{i}_{-s} \}; \quad \phi_u = \phi_u(i_{-s}) \\ \Psi_u &= w_1 \cdot k_{w1} \cdot \phi_u; \quad \underline{\Psi}_{us} = \Psi_u \cdot \frac{\underline{i}_{-s}}{i_{-s}} \end{aligned} \quad (6)$$

where:  $|\underline{\Psi}_{us}| = \Psi_u$  și  $|\underline{i}_{us}| = i_{-s}$ . Equations (6) have permitted construction of the structural diagram as in Fig.12 for modelling of core magnetization.

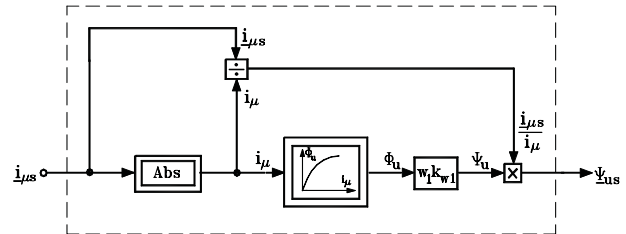


Figure 12: Model for “core magnetization”

Mathematically, the equations for the electromagnetic part (with saturated core) of an induction motor can be rewritten [3], [12], [13] as follow:

$$\begin{aligned} \underline{\Psi}_{ss} &= \int_0^t (\underline{u}_{ss} - R_s \cdot \underline{i}_{ss}) dt + \underline{\Psi}_{ss}(0) \\ \underline{\Psi}'_{rs} &= \int_0^t (0 - R'_r \cdot \underline{i}'_{rs} + j \cdot \omega_m \cdot \underline{\Psi}'_{rs}) dt + \underline{\Psi}'_{rs}(0) \end{aligned} \quad (7)$$

$$\underline{i}_{ss} = \frac{\underline{\Psi}_{ss} - \underline{\Psi}_{us}}{L_{s\sigma}}; \quad \underline{i}'_{rs} = \frac{\underline{\Psi}'_{rs} - \underline{\Psi}_{us}}{L'_{r\sigma}}$$

$$\underline{\Psi}_{us} = \Psi_u \cdot \frac{\underline{i}_{-s}}{i_{-s}}; \quad \underline{i}_{-s} = \underline{i}_{ss} + \underline{i}'_{rs}; \quad i_{-s} = \text{Abs} \{ \underline{i}_{-s} \}$$

$$\Psi_u = w_1 \cdot k_{w1} \cdot \phi_u; \quad \phi_u = f(i_{-s})$$

$$M = \frac{3}{2} \cdot p \cdot \text{Im} \{ \underline{i}_{-s} \cdot \underline{\Psi}_{ss}^* \} = \frac{3}{2} \cdot p \cdot \text{Im} \{ \underline{i}_{-s} \cdot \underline{\Psi}_{us}^* \}; \quad \omega_m = p \cdot \Omega_m$$

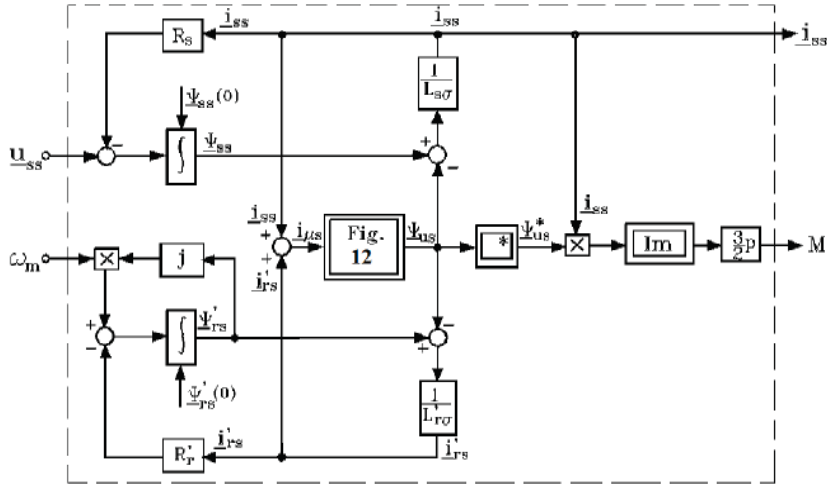


Figure 13: Structural diagram for the electromagnetic part of the induction motor (MAT)

Corresponding to equations (7), in Fig.13 it was built the structural diagram for the electromagnetic part of an induction motor of traction of an electric locomotive (MAT in Fig.3 and Fig.4). Here  $\underline{u}_{ss}$  (space phasor of the supply voltage) is the input variable. Output variables of the structural diagram from Fig.13 are the electromagnetic torque  $M$  (that determines the useful movement) and  $\underline{i}_{ss}$ . Note that all variables (except  $\omega_m$  and  $M$ ) are complex quantities in Fig.13.

**5. MODELLING OF SYNCHRONOUS MOTOR**

Synchronous motor is used on electric locomotive only by SNCF (BB 10004, BB 26000, TGV-A) in the electrical technology named "self-controlled synchronous motor" (SCSM, s. Fig.5). For modeling of the SCSM is proposed [3] decomposition of Fig. 14.

At modelling of the electromagnetic system of a synchronous motor (SM) is adopted the Park theory [10], [11], [14], [15] as in Fig.15.

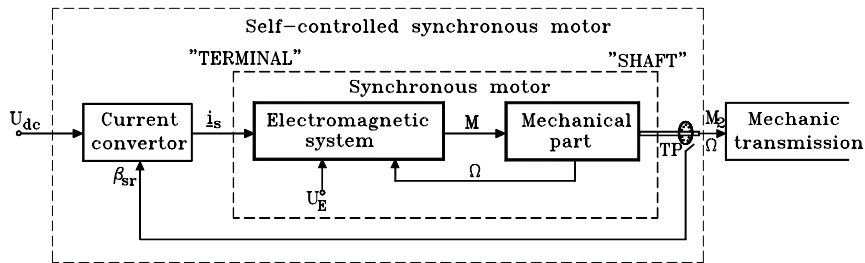


Figure 14: The "decomposition" of self-controlled synchronous motor (SCSM)

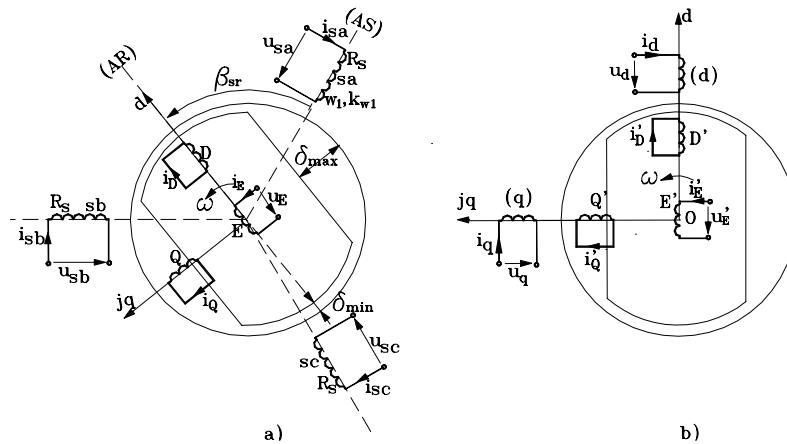


Figure 15: Electromagnetic system of synchronous motor  
a) in phase coordinates, b) Park model

The windings equations from transverse axis of the Park model of SM (with  $i_q$  as input variable) can be rewritten in the form:

$$\Psi'_Q = \int_0^t \left[ 0 - \frac{R'_Q}{L'_Q} \cdot \Psi'_Q + \frac{R'_Q}{L'_Q} \cdot L_{aq} \cdot i_q \right] dt + \Psi'_Q(0)$$

$$\Psi_q = \sigma_{qQ} \cdot L_q \cdot i_q + \frac{L_{aq}}{L'_Q} \cdot \Psi'_Q$$

$$i'_Q = \frac{\Psi'_Q}{L'_Q} - \frac{L_{aq}}{L'_Q} \cdot i_q$$
(8)

Equations (8) permit to build the structural diagram „Park transverse” for the electromagnetic part of SM as in Fig.16.

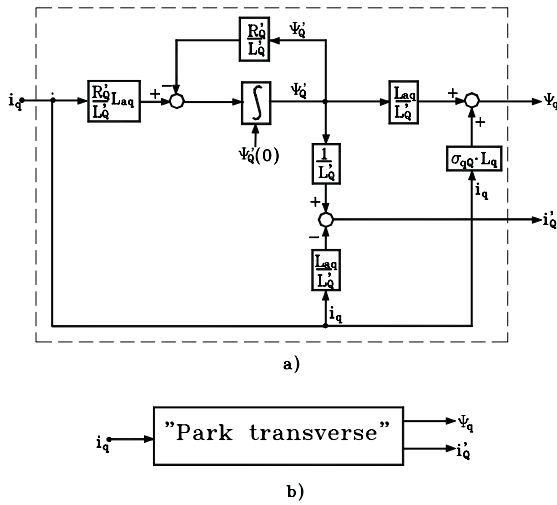


Figure 16: Structural diagram „Park transverse” for the electromagnetic part of SM

Absolutely similar, the windings equations from longitudinal axis of the Park model of SM (with  $i_d$  and  $u_E'$  as input variable) can be rewritten in the form:

$$\Psi'_D = \int_0^t \left[ 0 - \frac{R'_D}{L'_D} \cdot \Psi'_D + \frac{R'_D}{L'_D} \cdot L_{ad} (i_d + i'_E) \right] dt + \Psi'_D(0)$$

$$\Psi'_E = \int_0^t \left[ u'_E - \frac{R'_E}{L'_E} \cdot \Psi'_E + \frac{R'_E}{L'_E} \cdot L_{ad} (i_d + i'_D) \right] dt + \Psi'_E(0)$$

$$i'_D = \frac{\Psi'_D}{L'_D} - \frac{L_{ad}}{L'_D} \cdot (i_d + i'_E)$$

$$i'_E = \frac{\Psi'_E}{L'_E} - \frac{L_{ad}}{L'_E} \cdot (i_d + i'_D)$$
(9)

$$\Psi_d = -(1 - \sigma_{dE} - \sigma_{dD}) \cdot L_d \cdot i_d + \frac{L_{ad}}{L'_D} \cdot \Psi'_D + \frac{L_{ad}}{L'_E} \cdot \Psi'_E -$$

$$-(1 - \sigma_{dE}) \cdot L'_D \cdot i'_D - (1 - \sigma_{dE}) \cdot L'_E \cdot i'_E$$

Corresponding to above equations, in Fig.17 has been build the structural diagram named „Park longitudinal” for the electromagnetic part of SM.

By "assembling" structural diagrams from Fig. 16 and Fig.17 in correspondence with Park equations (10) is obtain the structural diagram "Park" (Fig.18) for the electromagnetic part of SM.

$$M = \frac{3}{2} \cdot p \cdot (\Psi_d \cdot i_q - \Psi_q \cdot i_d)$$

$$u_d = R_s \cdot i_d + \frac{d\Psi_d}{dt} - \omega \cdot \Psi_q$$

$$u_q = R_s \cdot i_q + \frac{d\Psi_q}{dt} + \omega \cdot \Psi_d$$

$$\omega = p \cdot \Omega = \frac{d\beta_{sr}}{dt}$$
(10)

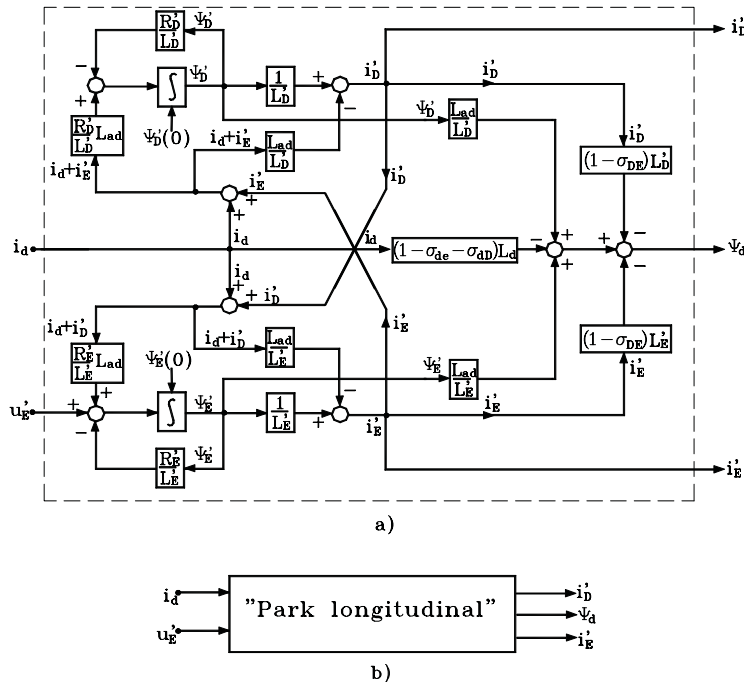


Figure 17: Structural diagram „Park longitudinal” for the electromagnetic part of SM

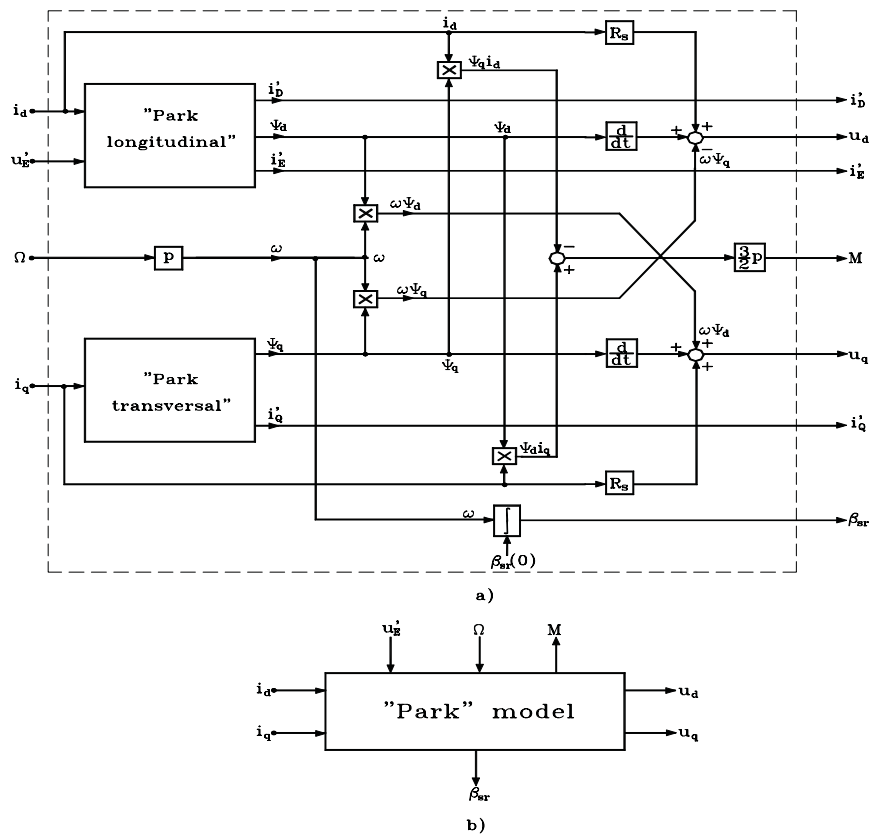


Figure 18: Structural diagram "Park" for the electromagnetic part of SM

That diagram is absolutely necessary for establish self-controlled synchronous motor model (SCSM, Fig.14) as traction motors.

### 6. NUMERICAL SIMULATION

The SIMULINK models corresponding to the presented structural diagrams can be easily implemented [9], [16].

For example, the SIMULINK model of the traction induction motor contains two blocks, corresponding to the electromagnetic part (MAT) and to the useful movement part (Fig. 19). Here the UM block contains the SIMULINK model of useful movement, based on structural diagram from Fig.6.

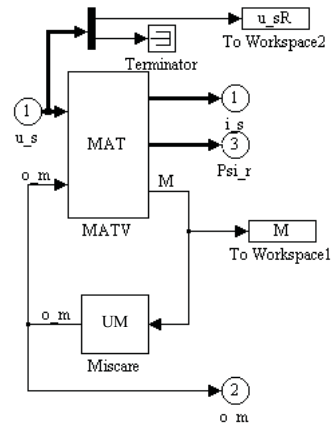


Figure 19: SIMULINK model of traction induction motor

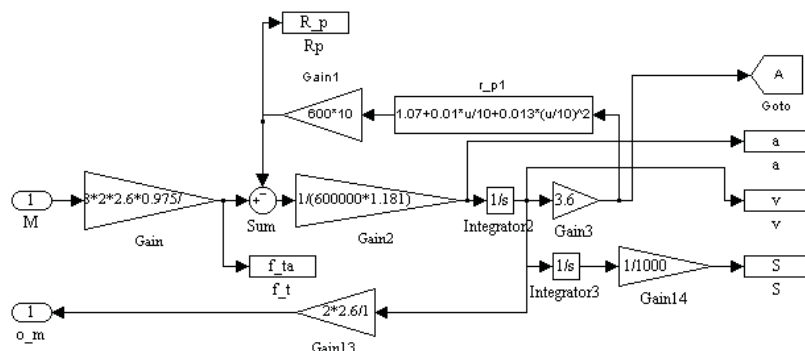


Figure 20: SIMULINK model of useful movement



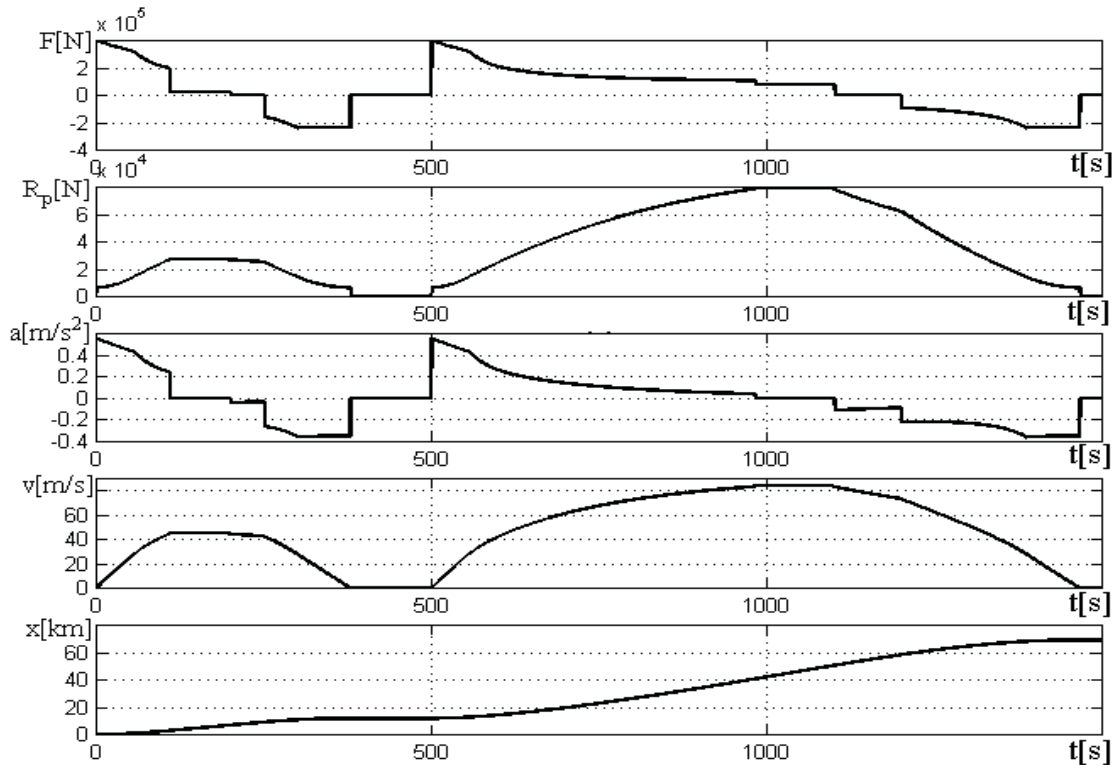


Figure 21: Running diagrams (numerical simulations) of ETR 500 high speed train

By means of this SIMULINK model (fig.19) they have been drawn the running diagrams corresponding to a test route of the ETR 500 high-speed train. They have been drawn the variations of the force, of the train resistance, of the acceleration, of the speed and of the distance (fig.21).

## 7. CONCLUSIONS

Article describes in a unified manner, modern modeling of electromechanical converters used on electric locomotives. For modelling is proposed the idea of fictitious decomposition (or split) of any traction electric motors in an electromagnetic part and in a mechanical part. Construction differences, functional differences and mathematical differences of the equations that describing the various types of electromechanical converters are given only by their electromagnetic parts.

Modeling was done by building structural diagrams that have shown the input variables, output variables and parameters (and characteristics) regardless of physical nature (electrical, magnetic or mechanical) of them. Structural diagrams can be easy converted into Simulink diagrams. By coupling (or interconnection) structural diagrams of traction equipment suitable electric power schemes can be easily established the models for any type of electric locomotive.

## References

- [1] D.A. Nicola, D.C. Cismaru, *Tracțiune electrică. Fenomene, Modele, Soluții, Vol. I*, Editura Sitech, Craiova, 2006.
- [2] R. Kaller, J.M. Allenbach, *Traction électrique I,II*, PPUR, Lausanne, 1995.
- [3] D.C. Cismaru, D.A. Nicola, Gh. Manolea, *Locomotive electrice. Rame și trenuri electrice*, Ed. Sitech, Craiova, 2009.
- [4] A. Steimel, *Electric Traction. Motion Power and Energy Supply Basics and Practical Experience*, Oldenbourg Industrieverlag, München, 2008.
- [5] F. Perticaroli, *Sistemi elettrici per i trasporti. Trazione elettrica*, Casa Editrice Ambrosiana, Milano, 2001.
- [6] V. Tulbure, G. Călin, *Locomotive cu motoare asincrone*, Editura Tehnică, București, 2004.
- [7] \*\*\* *Electric Traction Systems*, University of Warwick, UK, Fifth Residential Course Organised by IEE, 12-23 April, 1999.
- [8] \*\*\* *Electric Traction Systems* (The 9th Institution of Engineering and Technology Professional Development Course on), Manchester, UK, 6th-10th November 2006.

- [9] D.C. Cismaru, D.A. Nicola, Gh. Manolea, M.A. Drighiciu, C.A. Bulucea, *Mathematical Models of High-Speed Trains Movement*, WSEAS TRANSACTIONS on CIRCUITS and SYSTEMS, Issue 2, Volume 7, February 2008.
- [10] J. Chatelain, *Machines électriques*, PPUR, Lausanne, 1989.
- [11] T. Dordea, *Mașini electrice*, EDP București, 1977.
- [12] D.A. Nicola, D.C. Cismaru, *Structural Diagrams for Induction Machine*, Analele Universității din Craiova, Nr.20/1996.
- [13] D.A. Nicola, D.C. Cismaru, *Modelarea mașinii asincrone în tracțiunea electrică*, SIELMEC, Chișinău, 1997.
- [14] I. Boldea, *Transformatoare și mașini electrice*, EDP, București, 1994.
- [15] Chee-Mun Ong, *Dynamic Simulation of Electric Machinery Using Matlab/Simulink*, Prentice Hall Ptr, New Jersey, 1998.
- [16] D.C. Cismaru, D.A. Nicola, *Models of electric drives with traction induction motors used on locomotives fed from AC line*, CNAE, Craiova, 7-8 oct. 2010.